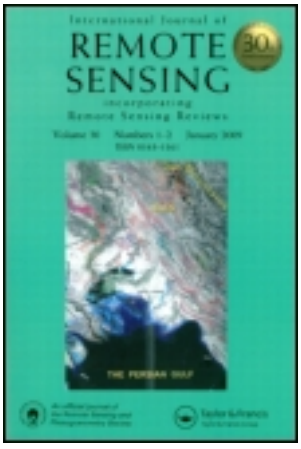

International Journal of Remote Sensing
Publication details, including instructions for authors and subscription information:
http://www.tandfonline.com/loi/tres20

Multi-temporal and multi-source cartography of the glacial cover of Nevado Coropuna (Arequipa, Peru) between 1955 and 2003

Walter Silverio [a] & Jean-Michel Jaquet [b]

[a] Climatic Change and Climate Impacts Research Group, Institute for Environmental Sciences, University of Geneva, CH-1227, Carouge, Geneva, Switzerland

[b] UNEP/DEWA-Europe/GRID-Geneva, CH-1219, Geneva, Switzerland

Available online: 05 Apr 2012

To cite this article: Walter Silverio & Jean-Michel Jaquet (2012): Multi-temporal and multi-source cartography of the glacial cover of Nevado Coropuna (Arequipa, Peru) between 1955 and 2003, International Journal of Remote Sensing, 33:18, 5876-5888

To link to this article: http://dx.doi.org/10.1080/01431161.2012.676742

International Journal of Remote Sensing
Vol. 33, No. 18, 20 September 2012, 5876–5888

Multi-temporal and multi-source cartography of the glacial cover of Nevado Coropuna (Arequipa, Peru) between 1955 and 2003

WALTER SILVERIO† and JEAN-MICHEL JAQUET*‡
†Climatic Change and Climate Impacts Research Group, Institute for Environmental Sciences, University of Geneva, CH-1227 Carouge, Geneva, Switzerland
‡UNEP/DEWA-Europe/GRID-Geneva, CH-1219 Geneva, Switzerland

(*Received 27 November 2009; in final form 6 February 2012*)

This study reports on the glacial cover evolution of the Nevado Coropuna between 1955 and 2003, based on Peruvian topographic maps and satellite images taken from the Landsat 2 and 5 multispectral scanner (MSS), Landsat 5 Thematic Mapper (TM) and Landsat 7 (ETM+). The normalized difference snow index has been applied to these images to estimate the glacierized area of Coropuna. The satellite-based results show that the glacier area was 105 ± 16 km^2 in 1975 (Landsat 2 MSS), which then reduced to 96 ± 15 km^2 in 1985 (Landsat 5 MSS), 64 ± 8 km^2 in 1996 (Landsat 5 TM) and 56 ± 6 km^2 in 2003 (Landsat 5 TM). Altogether, between 1955 and 2003, Coropuna lost 66 km^2 of its glacial cover, which represents a mean retreat of 1.4 km^2 year^{-1}, that is, a loss of 54% in 48 years (11% loss per decade). The maximum rate of retreat occurred during the 1980s and 1990s, a phenomenon probably linked with the pluviometric deficit of El Niño events of 1983 and 1992.

1. Introduction

According to the first glacier inventory of Peru, in 1970, the country had a glacial surface area of 2041.85 km^2, with Cordillera Ampato and Coropuna accounting for 146.73 and 82.6 km^2 (Hidrandina 1988) of the surface area, respectively, that is, 7.2% and 4.0% of the national glacial cover, respectively. Kaser and Osmaston (2002) reported that more than 70% of the tropical glacier areas (e.g. the Andes, East Africa and Irian Jaya, Indonesia) are concentrated in the Peruvian cordilleras.

At all latitudes, disregarding their type, glaciers are sensitive to climatic conditions (Hastenrath 1992, Sigurdsson and Jónsson 1995) and serve as indicators of regional climate change (Hall 2002). Globally, and with the exception of a few glaciers, mountain glaciers have been retreating since the end of the 'Little Ice Age' (Hall *et al*. 1995a). Following the more recent global climatic trend, tropical glaciers retreated substantially during the 1980s and 1990s (Kaser *et al*. 2003). This tendency was confirmed in the Peruvian tropical glaciers of the Cordillera Blanca (Silverio and Jaquet 2005).

*Corresponding author. Email: jean-michel.jaquet@unige.ch

International Journal of Remote Sensing
ISSN 0143-1161 print/ISSN 1366-5901 online © 2012 Taylor & Francis
http://www.tandfonline.com
http://dx.doi.org/10.1080/01431161.2012.676742

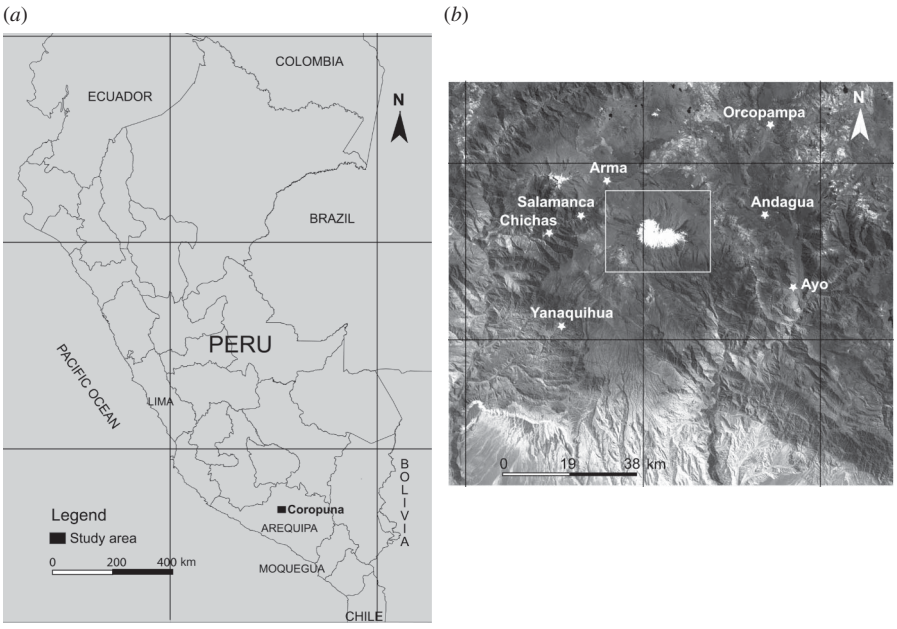

Figure 1. Location of the study site: (*a*) within the national territory of Peru; (*b*) part of the Landsat 5 TM image, band 2, 4 September 2003, with the climate stations around Coropuna (white frame) (georeferenced to the Universal Transverse Mercator, zone 18 south).

The glaciers of Nevado Coropuna represent the most important freshwater 'reservoirs' for the Arequipa region (figure 1(*a*)). The melting of the glaciers mitigates the lack of water during the dry season or possible abnormal climatic events (Peduzzi *et al*. 2010). Francou and Wagnon (1998) reported that the disappearance of Coropuna would result in the loss of a fundamental water resource, used for farming activities and water supply to the cities.

In Peru, the last decades of the twentieth century were marked by demographic growth, coinciding with a reduction in hydrological reserves. During the same period, there was an increased demand for drinking water for the population and for other activities (irrigation, hydroelectric power, etc.), causing conflicts between users. To quote one example, between autumn 2003 and winter 2004, the regions of Arequipa and Moquegua, located in southern Peru (figure 1(*a*)), experienced tensions for the control of the water reserves of the Tambo Grande dam. Fortunately, this conflict was diffused by central government negotiation. This tense context thus justifies the need for carrying out an inventory of the available hydrological resources and for planning of their long-term management in the perspective of sustainable development.

This study is part of the project, *Impact assessment of climatic change on Coropuna glacier (Peru) and related threats to water supplies*, carried out in collaboration with the German Cooperation Programme (GTZ), the University of Geneva and UNEP/GRID-Europe. We present our results and discuss the approach used for the multi-temporal and multi-data mapping of the Coropuna glaciers, between 1955 and 2003. In addition, analyses are made based on precipitation data obtained from the weather station in the Coropuna region as well as El Niño events of 1983 and 1992.

2. Study area

Nevado Coropuna is located between 15° 25′–15° 38′ S latitude and 72° 29′–72° 46′ W longitude in the Cordillera Ampato (Peruvian State of Arequipa; figure 1(*a*)). The Coropuna massif is approximately 15 km long from east to west and 8 km wide from north to south (figure 1(*b*)). It includes several summits that exceed 6000 m above sea level, with its highest peak reaching 6425 m.

The topographic aspect of Nevado Coropuna is characterized by rather moderate slopes (figure 4). The glacier is located on the divide between the Rio Arma and Rio Majes watersheds (Hidrandina 1988, part 2, p. 32) and drains entirely into the Pacific Ocean (Morales Arnao 1998). Its meltwater is used mainly for agriculture and drinking purposes.

The study conducted by Hidrandina (1988), based on aerial photographs taken in June 1962, showed that Coropuna consisted of 17 glaciers covering an area of 82.6 km^2 (figure 4). Peduzzi *et al*. (2010), however, reported that the area of the glaciers was reduced to 48.1 km^2 in 2008.

In the vicinity of tropical glaciers, the climate of the region is characterized by relatively large daily temperature ranges but small seasonal variations (Kaser and Osmaston 2002). In the Andes, most of the rain falls between December and April, with maximum rainfall during March and February in the north and south, respectively (Rome-Gaspaldy and Ronchail 2005). In the Coropuna region, the dry season is between May and September, when it rarely rains (Herreros *et al*. 2009).

3. Data

Although several types of satellite data are available for snow cover mapping (e.g. the Moderate Resolution Imaging Spectroradiometer (MODIS), the Advanced Very High Resolution Radiometer (AVHRR) and the Special Sensor Microwave Imager (SSM/I)), their resolution is too coarse for our purpose, which is why we have chosen to work on Landsat imagery (table 1). All images were carefully screened for the presence of thick and thin clouds by visual interpretation and using the criteria given by Dozier (1989) and Riggs and Hall (2002). Three images were provided by UNEP/GRID/DEWA-Sioux Falls (USA). The first image was taken from Landsat 2 multispectral scanner (MSS) on 30 July 1975 with a spatial resolution of 57 m. There are some linear artefacts in the data which, however, do not affect the Coropuna mountain range. The second image was taken from Landsat 5 MSS on 1 August 1985 with a resolution of 57 m. The third image was taken from Landsat 5 Thematic

Table 1. Satellite images.

Type	Date	Resolution (m) Path/row	Solar elevation angle (°)	Format	Georeference	Fresh snow cover
Landsat 2 MSS	30 July 1975	57 03/071	36.7	NLAPS	UTM	No
Landsat 5 MSS	1 August 1985	57 04/071	39.3	NLAPS	UTM	No
Landsat 5 TM	31 August 1996	28.50 04/071	43.0	GeoTIFF	UTM	Some
Landsat 7 ETM+	21 June 2002	30 04/071	39.4	GeoTIFF	Geographic then UTM	Yes
Landsat 5 TM	4 September 2003	30 04/071	49.2	GeoTIFF	UTM	No

Table 2. Location of the climate stations in the Coropuna region (see also figure 1(*b*)).

Station	Latitude (South)	Longitude (West)	Altitude (m)	Period of observation	From Coropuna main summit	
					Distance (km)	Direction
Andagua	15° 29′ 36″	72° 20′ 56″	3587	1968–2003	30	E
Arma	15° 24′ 30″	72° 46′ 00″	4270	1964–1986	20	NW
Ayo	15° 40′ 44″	72° 16′ 12″	1956	1968–2003	42	E-SE
Chichas	15° 32′ 40″	72° 54′ 59″	2120	1972–2003	30	W
Orcopampa	15° 15′ 38″	72° 20′ 19″	3779	1965–2003	45	NE
Salamanca	15° 30′ 00″	72° 50′ 00″	3203	1972–2003	22	W-NW
Yanaquihua	15° 46′ 59″	72° 52′ 56″	3130	1973–1997	37	SW

Mapper (TM) on 31 August 1996 with a resolution of 28.5 m. The first two images were taken without clouds being visible, whereas in the third image (31 August 1996) some snow spots in the zones surrounding the Coropuna glaciers were visible, which were due to the passage of a storm. Similarly, GTZ-Peru provided an image of Landsat 7 Enhanced Thematic Mapper Plus (ETM+) taken on 21 June 2002 with a resolution of 30 m. It was georeferenced (WGS84) and geometrically corrected using a topographic map (1:100 000 scale) of the National Geographical Institute (IGN) of Peru. Clouds, which cover a part of the Nevado Coropuna glaciers, as well as fresh snow cover are visible in the image. The last Landsat 5 TM image (path/row 04/071; 30 m resolution), acquired on 4 September 2003, was provided by the National Institute for Space Research (INPE, Brazil). Since the image was taken at the end of the dry season, its quality is optimal (containing neither clouds nor fresh snow).

The digital topographic map was provided by the IGN of Peru. It includes two sheets of national cartography at a scale of 1:100 000 (Cotahuasi: 31-Q and Chuquibamba: 32-Q). The map was compiled by stereo-photogrammetric methods from aerial photos taken on 15 July 1955. The original layers were georeferenced into the geographic coordinate system (latitude/longitude) and contained the topographic contour lines (50 m level) that discriminate the glacier and nonglacier areas. No debris-covered glaciers were identified on these maps.

In the Coropuna region, there are 14 weather stations. However, for half of them, the records were not continuous and sometimes measurements were available only for a brief period. Leaving these out, we analysed the precipitation data for the remaining seven stations, with monthly data available for over 20 years or more (figure 1(*b*)): Andagua, located 30 km east from the main Coropuna summit; Arma, at 20 km NW; Ayo, at 42 km E-SE; Chichas, at 30 km W, Orcopampa, at 45 km NE; Salamanca, at 22 km W-NW and Yanaquihua, at 37 km SW (see table 2). The evolution of mean annual precipitation between 1964 and 2000 is shown graphically in figure 2.

4. Methodology

4.1 *Pretreatment*

The topographic map was reprojected onto the universal transverse mercator (UTM) coordinate system (zone 18, south) prior to on-screen digitizing of the glaciers' limits for 1955. Because of the suspected presence of fresh snow, the June 2002 image

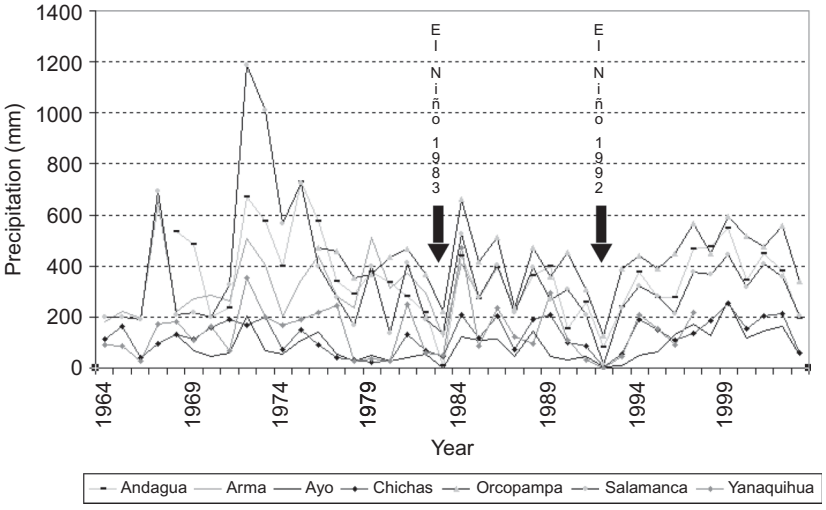

Figure 2. Evolution of mean annual precipitation at the climate stations of Coropuna region. The deficit in precipitation during the 1983 and 1992 El Niño events is clearly shown (see also table 5).

Table 3. Image geometric correction and RMS errors.

Image (date)	Image for resample	Resolution (m)	RMS error (pixels)
MSS 30 July 1975	1 August 1985	57	1.0
MSS 1 August 1985	21 June 2002	57	1.4
TM 31 August 1996	21 June 2002	30	3.0
TM 4 September 2003	21 June 2002	30	3.4

was not considered for further analysis. Instead, it was reprojected onto the UTM coordinate system (zone 18, south) and used as a template for the geometric correction of the other images because the topographic maps were not all available for that purpose. Geometric correction was performed on subimages covering Coropuna (30 km × 23 km), using seven control points, a first-degree polynomial transformation and nearest-neighbour resampling. Considering the relative inaccuracy of the 1:100 000 scale map used for geo-correction of the June 2002 image, the root mean square (RMS) errors (table 3) were acceptable.

4.2 *Mapping of the glacial extent*

4.2.1 Topographic map. The glacier limits were manually delineated by on-screen digitizing, resulting in a polygon of surface area S. The uncertainty affecting the glacier area S was estimated by rasterizing the vector limit at a resolution of 100 m and computing the surface area s of this strip, yielding the expression $S \pm s$ (see figure 3).

4.2.2 MSS images. Since the MSS does not have the same radiometry as the TM, the normalized difference snow index (NDSI) could not be applied to map glacier limits for the 1975 and 1985 images. For these years, the glacial surface was obtained by a manual delineation on the MSS colour composite (bands 1, 2 and 4). The uncertainty

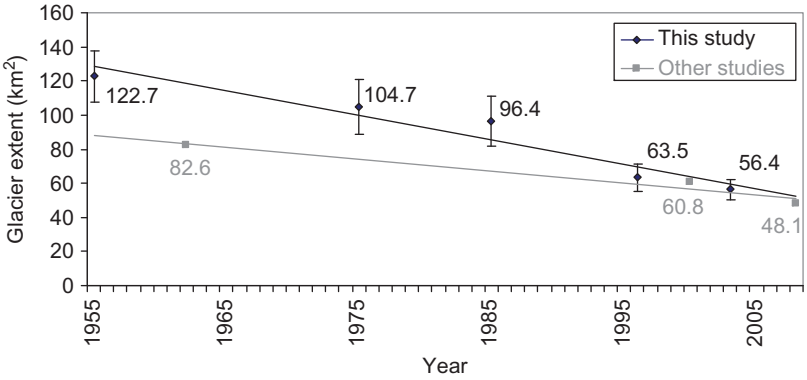

Figure 3. Evolution of glacial cover of Coropuna between 1955 and 2003 from various sources: this study, with uncertainty bar; 1962: Hidrandina (1988); 2000: Racoviteanu *et al*. (2007); 2008: Peduzzi *et al*. (2010). Trends plotted by hand.

for these years was also calculated by vector/raster conversion of the glacier margin, this time at a resolution of 57 m (see figure 3).

4.2.3 TM images. The radiometric characteristics as well as the glaciological applications of Landsat TM images have been described by several authors (Dozier and Marks 1987, Hall *et al*. 1987, Dozier 1989). Indices or spectral-band ratios are known for their ability to eliminate, or at least to minimize, illumination differences due to topography (shading of a surface caused by solar illumination angle and slope orientation; Colby 1991). These ratios were calculated from visible and near-infrared channels with low correlation and, ideally, after elimination of additive noise (Bonn and Rochon 1993). Since haze was not visible on the images, this last treatment was not deemed necessary (Silverio and Jaquet 2003).

In order to have an optimal representation of the Coropuna high-altitude land-cover themes between 1996 and 2003, ranging from pure ice to rock outcrops, we used the NDSI. It can be determined from digital numbers of two TM bands using the following equation (Hall *et al*. 1995b):

$$\mathrm{NDSI} = \frac{((\text{TM band 2}) - (\text{TM band 5}))}{((\text{TM band 2}) + (\text{TM band 5}))}. \tag{1}$$

The NDSI allows a spectral discrimination between snow, soil, rock and cloud cover (Dozier 1989). Sidjak and Wheate (1999) demonstrated that this index is efficient for snow mapping in rough topography. Silverio and Jaquet (2003, 2005) have shown the effectiveness of the NDSI for glacial cartography in the tropical Andes (Cordillera Blanca, Peru). The NDSI provides a sharp image of the boundary between the glacier terminus and the surrounding moraine; it also permits a fairly accurate inter-comparison of the bare ice part of the glacier tongue positions in different years (Hall *et al*. 2001).

Normally, the NDSI values vary between −1 and +1. The values we computed for the 1996 and 2003 TM images are located within this interval (see table 4). We tested several threshold values to achieve an optimal mapping of glacier limits and selected

Table 4. Spatial differentiation of glacier entities for 1996 and 2003 based on the NDSI.

Year	NDSI value range	NDSI criterion for glacier limits
1996	−0.33 to +0.93	NDSI ≥ 0.47
2003	−0.70 to +1.00	NDSI ≥ 0.39

those reported in table 4 because they gave the best match with the glacier limits seen on the colour composite image. In 1996, the chosen threshold (0.47) was higher because there was some amount of fresh snow on the glaciers (Hall *et al*. 1992).

Glacier (*bare ice*) delineation is based on a methodology detailed in Silverio and Jaquet (2003, 2005): the NDSI images were segmented using the criteria given in table 4 (last column). The margins of glaciers were obtained by raster/vector conversion (Silverio and Jaquet 2003).

Rock outcrops located inside the glaciers were also mapped by NDSI using the criterion given in table 4 (Silverio and Jaquet 2009). The rock outcrop area was subtracted from the total surface.

The cartographic uncertainty on glacier area S was estimated by computing the surface area s of the rim of 30 m pixels bordering the glacier, yielding the expression $S \pm s$ (see figure 3) (Silverio and Jaquet 2005).

5. Results

5.1 *Glacial cover*

The results of the study show that in 1955, the total glacial surface area obtained from the topographic map of Nevado Coropuna was 123 ± 15 km^2. According to the satellite imagery, the total glacial areas of Nevado Coropuna in 1975, 1986, 1996 and 2003 were 105 ± 16, 96 ± 15, 64 ± 8 and 56 ± 6 km^2, respectively (see figure 3). Coropuna lost an area of 18 km^2 (with a mean retreat of 0.9 km^2 year^{-1}) between 1955 and 1975, of 8.3 km^2 (0.8 km^2 year^{-1}) between 1975 and 1985, of 32.9 km^2 (3 km^2 year^{-1}) between 1985 and 1996 and of 7 km^2 (1 km^2 year^{-1}) between 1996 and 2003.

Thus, the total loss of the glacial cover of Coropuna between 1955 and 2003 was 66.3 km^2 (54% of the original figure of 1955) with a mean retreat of 1.4 km^2 year^{-1}. Furthermore, the maximum reduction in the glacier area was observed during the period of 1985–1996.

5.2 *Precipitation*

Annual precipitation is variable and strongly depends on the location of the climate stations (table 5). During 1983 and 1992, corresponding to El Niño events, the volume of precipitation shows a deficit at all the stations of the Coropuna region (see the arrows in figure 2). This was observed elsewhere in the Andes, together with high air temperatures, low wind speed and reduced cloud cover, inducing a lower glacier albedo and a corresponding stronger ablation (Francou *et al*. 2004).

Table 5. Precipitation in the Coropuna region during the 1983–1998 El Niño events.

Station	Mean annual precipitation (mm)	Precipitation during El Niño 1983 event (mm) (and deficit)	Precipitation during El Niño 1992 event (mm) (and deficit)	Precipitation during El Niño 1998 event (mm) (with difference from mean)
Andagua	357.4	7 (−98%)	80 (−78%)	474 (+32.5%)
Arma	318.0	121 (−62%)	N/A	N/A
Ayo	85.4	0 (−100%)	4 (−94%)	129 (+51%)
Chichas	123.7	45 (−64%)	5 (−96%)	186 (+50%)
Orcopampa	423.2	221 (−48%)	129 (−70%)	448 (+6%)
Salamanca	349.2	137 (−61%)	13 (−96%)	365 (+5%)
Yanaquihua	143.3	51 (−64%)	0.4 (−99.7%)	N/A

6. Discussion

Figure 3 clearly illustrates the general retreat of the Coropuna glaciers. It is evident that they have been shrinking since the 1950s with a total decrease of approximately 54% in the glaciated area over a period of 48 years (see figure 4).

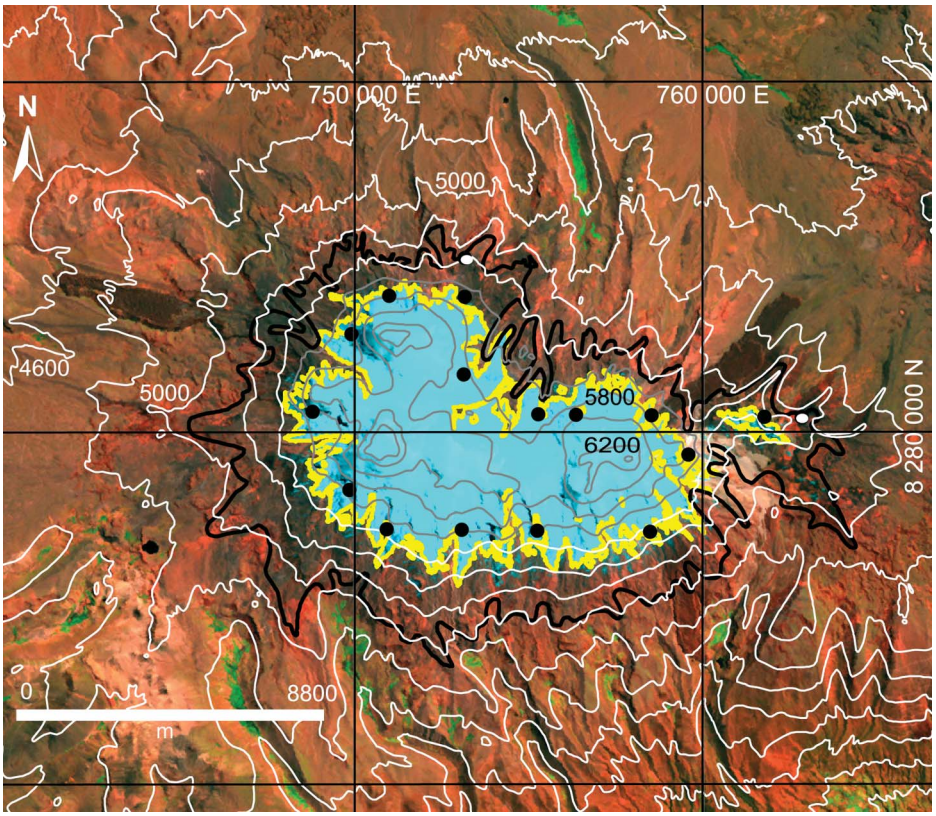

Figure 4. Nevado Coropuna glacial cover between 1955 (black limit) and 2003 (yellow limit). Topographic contours (white and grey) are spaced 200 m apart. Black and white dots represent the location of the glaciers surveyed in 1962 by Hidrandina (1988).

Since satellite images were registered with topographic maps at a scale of 1:100 000 (with an accuracy of about ±100 m), the study results must, therefore, be considered at a similar scale, in spite of the higher pixel resolution of the images (30 and 57 m).

The monitoring accuracies of the position of the glacial tongue front, using traditional cartographic methods (theodolite) and photogrammetry, are ±5 and ±10 m, respectively (Sturm *et al*. 1991). For satellite imagery, this accuracy is limited by the sensor resolution: approximately 57 m for Landsat MSS and 30 m for Landsat TM (Hall *et al*. 1992, 1995a, Williams *et al*. 1997).

Notwithstanding the limited accuracy of the glacial cover from the topographical map, we consider our results for 1955 to be acceptable. According to Ames (pers. comm., 27 August 2004), the IGN map was based on the analysis of aerial photographs of 15 July 1955 taken after the passage of a storm, known in the Andes as 'bad weather'. In the Andes, during 'bad weather', snow can fall even outside the margins of glaciers, but it will remain on the surface only for a few days. At high altitudes, snow will stay longer and will be able to feed the renewal of the glaciers and can also cover the rock outcrops. It is undoubtedly as a result of the said phenomenon that during the production of the topographic map, the IGN did not locate the rock outcrops. Consequently, it is assumed that the glacial surface for 1955 may have been overestimated with an uncertainty of ±100 m around the external margins, resulting in a glaciated area of 123 ± 15 km^2, or 123 km^2 ±12%.

According to Ames (pers. comm., 27 August 2004), the cartographic representation of glaciers is somewhat inaccurate. (During the first glacier inventory of Peru, the area given was 82.6 km^2 (see figure 3).) Not knowing the uncertainty for the year 1962, and also since the method used was different from ours, we cannot compare their levels of accuracy.

Concerning the years 1975 and 1985, the satellite images were taken, respectively, at the end of July and at the beginning of August, the ideal period for glacial cartography in the Andes. In spite of the relatively low resolution of the images, we consider that our results are acceptable. The glacial margin with a reliability of ±1 pixel for the image date gives an uncertainty band of 57 m around the external limit. For these years, the uncertainty represents ±16 km^2 (±15%) and ±15 km^2 (±16%), respectively.

In 1996, the rather high value of NDSI (≥0.47, see table 4) suggests that the imagery was taken after the passage of 'bad weather'. Normally, at the end of August, the reflectance should be lower since, for this date, the snow that had fallen during the preceding winter had time to melt and left only the 'bare ice'. Despite these disadvantages, we consider our results to be valid because the NDSI clearly discriminates ice and non-ice. As in previous cases, the estimated glacier limit is reliable at ±1 pixel. Taking into account the ±30 m approximation leads to an uncertainty of ±8 km^2 (±13%).

Since in 2003 the satellite images were acquired in September, the determination of glacier margins can be expected to provide optimal results. Snow fallen the year before had had time to melt, leaving only bare ice in the ablation area of the glaciers. This ice has a much lower reflectance (Hall *et al*. 1992), which explains the low NDSI value (0.39, table 3). Ice and non-ice are then clearly delineated using the NDSI. As in previous cases, the glacier limit estimate is reliable within ±1 pixel. Taking into account the ±30 m approximation, the uncertainty is ±6 km^2 (±11%).

For 1996 and 2003, we did not discriminate subclasses such as ice and snow of different textures (see Hall *et al*. (1987, 1988) and Williams *et al*. (1991)) because

our principal objective was to estimate the total glacial cover of Coropuna: in this mountain range, there are no glaciological field measurements to confirm the results obtained by the analysis of the satellite images.

Owing to the relatively large uncertainty attached to the 1955–1985 glacial cover estimates, the differences between pairs of values during this time span cannot be proven to be *statistically* significant. However, considering the entire study period (1955–2008), the decreasing trend is obvious. This is particularly valid between 1996 and 2008, when our estimates are confirmed by Racoviteanu *et al*. (2007), who gave a surface of 60.8 km^2 for 2000 (according to the interpretation of a 15 m ASTER image), and by Peduzzi *et al*. (2010), who estimated that in 2008 the Coropuna glacial cover was 48.1 km^2 (figure 3, 'Other studies').

Keeping in mind these caveats, the mean average retreat of Coropuna was of the order of 0.9 km^2 $year^{-1}$ between 1955 and 1985, 3 km^2 $year^{-1}$ between 1985 and 1996 and about 1 km^2 $year^{-1}$ between 1996 and 2003. Hence, a more significant retreat seems to have taken place between 1985 and 1996 (clearly visible in figure 3). This tendency was also observed in Cordillera Blanca between 1987 and 1996 (Silverio and Jaquet 2005), indicating that in the Peruvian tropical Andes, an 'acute retreat' of the glaciers occurred during the 1980s and 1990s.

Figure 2 clearly shows that for the 1983 and 1992 events, there was a considerable deficit of precipitations at all the stations around Coropuna. The deficit varies between 48% and 100% for 1983 and between 70% and 100% for 1992 (see table 5). These years correspond to the El Niño–Southern Oscillation (ENSO) events with strong intensity (Herreros *et al*. 2009). In general, during El Niño, precipitations drop by 10–30% (IRD 2005a) in the Andes. Indeed, several authors have observed a deficit of precipitation in the Peruvian southern Andes during El Niño events (Aceituno and Montecinos 1993, Garreaud *et al*. 2003, Rome-Gaspaldy and Ronchail 2005, Herreros *et al*. 2009). However, these pluviometric deficits were variable during the events and among stations (Lagos *et al*. 2008). During the 1998 El Niño event, precipitation was variable (Herreros *et al*. 2009) in five of the seven weather stations, where between 5% and 51% *excess* precipitation was observed (see table 5). Clearly, attempting to typify precipitation during El Niño events in the Coropuna region is a difficult exercise. In addition, it is necessary to emphasize that excess precipitation does not necessarily imply a glacial advance or a positive accumulation because the precipitation on the glacier may be rain (Francou *et al*. 2004). At this stage, we can only hypothesize a causal link between the 1983 and 1992 precipitation deficits and the accelerated decrease in glacial cover between 1985 and 1996.

In the tropical Andes, since 1939, temperatures have increased by 0.10°C per decade. In the last 25 years, these values have been multiplied by 3, resulting in an increase of 0.32–0.34°C per decade (Vuille and Bradley 2000, Vuille *et al*. 2003). According to Vuille and Bradley (2000), the increase in temperature could be related to the El Niño phenomenon, which would imply a glacial retreat in the tropical Andes. Indeed, during El Niño events, the limit between rain and snow on the glaciers rises by 200–300 m as a consequence of a 1–2°C heating of the atmosphere (Francou *et al*. 2004, IRD 2005a,b), thus inducing a deficit in snow alimentation.

During El Niño events, the mass balance of the glaciers in the tropical Andes is negative, while during La Niña events (the cold phase of ENSO), the ablation is reduced, and thus the glaciers tend to remain stable or even to advance (Francou *et al*. 2003, 2004, IRD 2005b).

7. Conclusions

In spite of the limited accuracy, the topographic maps at the 1:100 000 scale are able to represent the state of the glaciers for a given date. Similarly, MSS images with a 57 m resolution can display the general state of the glaciers. As such, these low-resolution data provide a baseline of climate change effects for the period prior to the availability of high-resolution satellite images. In this study, TM images with a resolution of 30 m yielded the best results and offer a great potential to map glacial retreat in the Andes (Silverio and Jaquet 2005).

It would be ideal that the results obtained by the satellite imagery analysis be confirmed by field measurements, as done elsewhere (see Williams *et al*. (1997)). However, in a country like Peru, it is difficult to make direct field glaciological measurements in all parts of the cordilleras because the glaciers are located in remote regions, and there is a chronic lack of financial and technical resources to carry out such tasks.

The results obtained by multi-source analysis reflect the state of a glacier, driven by the general tendency of the climate. Multi-source cartography is a tool that makes it possible to have a general vision of the space–time distribution of the hydrological reserves in a region. To be useful, the results obtained should be integrated within a geographical information system (GIS) (Silverio 2001, Paul 2003). Associated with socio-economic data within a GIS, the glacial cover map can thus contribute to land management and decision-making.

Between 1955 and 2003, Coropuna lost 54% of its glacial cover. In the 1980s and 1990s, there was a very marked retreat, possibly due to the deficit of precipitation during the 1983 and 1992 El Niño events. This causal link with the El Niño phenomenon, combined with a rise in temperature, has been postulated elsewhere in the Andes (Francou *et al*. 2003, IRD 2005b): the glaciers have a maximum ablation (negative mass balance) during an El Niño episode or immediately after the event. During La Niña events, the phenomenon is reversed: glaciers remain stable or even advance. These hypotheses should be tested on the basis of more frequent glacial cover maps during the 1980s and 1990s, as well as mass balance calculations when feasible.

Acknowledgements

This study was supported by the GTZ. We thank Josef Haider and Juan Carlos Montero of Cooperación Peruana Alemana para la Seguridad Alimentaria (COPASA, Arequipa-Peru) and Monika Kiene of GTZ (Lima, Peru) for their help. We offer our gratitude to Mark A. Ernste, former collaborator of the UNEP/GRID-Sioux Falls (DEWA), USGS EROS Data Center, SD, USA, for providing the 1975, 1985 and 1996 satellite images. We also extend our thanks to Pascal Peduzzi and Christian Herold, UNEP/GRID-Europe, for their help. Special thanks to Martin Beniston, University of Geneva, and to anonymous reviewers, whose comments helped to improve earlier versions of this article.

References

Aceituno, P. and Montecinos, A., 1993, Análisis de la estabilidad de la relación entre la oscilación del sur y la precipitación en América del Sur. *Bulletin De L'institut Français D'études Andines*, **22**, pp. 53–64.

Bonn, F. and Rochon, G., 1993, *Précis de Télédétection, Volume 1: Principes et Méthodes* (Sainte-Foy: Presses de l'Université de Québec et AUPELF).

Colby, J.D., 1991, Topographic normalization in rugged terrain. *Photogrammetric Engineering and Remote Sensing*, **57**, pp. 531–537.

Dozier, J., 1989, Spectral signature of Alpine snow cover from Landsat Thematic Mapper. *Remote Sensing of Environment*, **28**, pp. 9–22.

Dozier, J. and Marks, D., 1987, Snow mapping and classification from Landsat Thematic Mapper. *Annals of Glaciology*, **9**, pp. 97–103.

Francou, B., Vuille, M., Favier, V. and Cáceres, B., 2004, New evidence for an ENSO impact on low-latitude glaciers: Antizana 15, Andes of Ecuador, 0°20′ S. *Journal of Geophysical Research*, **109**, pp. 1–17.

Francou, B., Vuille, M., Wagnon, P., Mendoza, J. and Sicart, J.-E., 2003, Tropical climate change recorded by a glacier in the central Andes during the last decades of the twentieth century: Chacaltaya, Bolivia, 16°S. *Journal of Geophysical Research*, **108**, 4154, doi:10.1029/2002JD002959.

Francou, B. and Wagnon, P., 1998, *Cordillères Andines, Sur Les Hauts Sommets De Bolivie, Du Pérou Et D'equateur* (Grenoble: Glénat).

Garreaud, R., Vuille, M. and Clement, A.C., 2003, The climatic of the Altiplano: observed current conditions and mechanisms of past changes. *Palaeogeography, Palaeoclimatology, Palaeoeology*, **194**, pp. 5–22.

Hall, D., 2002, Monitoring glacier changes from space. Available online at: http://www.isset.org/site_of_the_month/glacier_bay/hall.science.txt.html (accessed 9 February 2011).

Hall, D.K., Bayr, K., Bindschadler, R.A. and Schöner, W., 2001, Changes in the Pasterze Glacier, Austria, as measured from the ground and space. In *58th Eastern Snow Conference*, 14–17 May 2001, Ottawa, ON. Available online at: http://www.easternsnow.org/proceedings/2001/Hall_1.pdf (accessed 9 February 2011).

Hall, D.K., Benson, C.S. and Field, W.O., 1995a, Changes of Glacier Bay, Alaska, using ground and satellite measurements. *Physical Geography*, **16**, pp. 27–41.

Hall, D.K., Chang, A.T.C. and Siddalingaiah, H., 1988, Reflectances of glaciers as calculated using Landsat-5 Thematic Mapper data. *Remote Sensing of Environment*, **25**, pp. 311–321.

Hall, D.K., Ormsby, J.P., Bindschadler, R.A. and Siddalingaiah, H., 1987, Characterization of snow and ice reflectance zones on glacier using Landsat Thematic Mapper data. *Annals of Glaciology*, **9**, pp. 104–108.

Hall, D.K., Riggs, G.A. and Salomonson, V.V., 1995b, Development of methods for mapping global snow cover using Moderate Resolution Imaging Spectroradiometer (MODIS) data. *Remote Sensing of Environment*, **54**, pp. 127–140.

Hall, D.K., Williams Jr., R.S. and Bayr, K., 1992, Glacier recession in Iceland and Austria. *EOS (Transactions American Geophysical Union)*, **73**, pp. 129–141.

Hastenrath, S., 1992, Greenhouse indicators in Kenya. *Nature*, **355**, pp. 503–504.

Herreros, J., Moreno, I., Taupin, J.-D., Ginot, P., Patris, N., De Angelis, M., Ledru, M.-P., Delachaux, F. and Schotterer, U., 2009, Environmental records from temperate ice on Nevado Coropuna saddle, southern Peru. *Advances in Geosciences*, **22**, pp. 27–34.

Hidrandina, S.A. and Unit of Glaciology and Hydrology Huaraz, 1988, *Glacier Inventory of Peru* (Lima: Consejo Nacional de Cience y Tecnología (CONCYTEC)).

IRD (Institut de Recherche pour le Développement), 2005a, El Niño et la fonte des glaciers dans les Andes tropicales. Available online at: http://www.ird.fr/la-mediatheque/fiches-d-actualite-scientifique/208-el-nino-et-la-fonte-des-glaciers-dans-les-andes-tropicales (accessed 9 February 2011).

IRD (Institut de Recherche pour le Développement), 2005b, Petits glaciers des Andes tropicales: une disparition annoncée. Available online at: http://www.ird.fr/la-mediatheque/fiches-d-actualite-scientifique/127-petits-glaciers-des-andes-tropicales-une-disparition-annoncee (accessed 9 February 2011).

Kaser, G., Juen, I., Georges, C., Gomez, J. and Tamayo, W., 2003, The impact of glaciers on the runoff and the reconstruction of mass balance history from hydrological data in the Cordillera Blanca, Perú. *Journal of Hydrology*, **282**, pp. 130–144.

Kaser, G. and Osmaston, H., 2002, *Tropical Glaciers* (Cambridge: Cambridge University Press).

Lagos, P., Silva, A., Nickl, E. and Mosquera, K., 2008, El Niño – related precipitation variability in Perú. *Advances in Geosciences*, **14**, pp. 231–237.

Morales Arnao, B., 1998, Glaciers of Perú, with sections on the Cordillera Blanca on Landsat Imagery and Quelcaya ice cap, by Hastenrath, S. In *Satellite Image Atlas of Glaciers of the World, South America, U.S. Geological Survey Professional Paper 1386-I-4*, R.S. Williams Jr. and J.G. Ferrigno (Eds.), pp. 151–179 (Washington, DC: United States Government Printing Office).

Paul, F., 2003, The new Swiss glacier inventory 2000. Application of remote sensing and GIS. PhD thesis, University of Zurich, Switzerland.

Peduzzi, P., Herold, C. and Silverio, W., 2010, Assessing high altitude thickness, volume and area changes using field, GIS and remote sensing techniques: the case of Nevado Coropuna (Peru). *The Cryosphere*, **4**, pp. 313–323. Available online at: http://www.the-cryosphere.net/4/313/2010/tc-4-313-2010.pdf (accessed 10 February 2011).

Racoviteanu, A.E., Manley, W.F., Arnaud, Y. and Williams, M.W., 2007, Evaluating digital elevation models for glaciologic applications: an example from Nevado Coropuna, Peruvian Andes. *Global Planetary Change*, **59**, pp. 110–125.

Riggs, G. and Hall, D.K., 2002, Reduction of cloud obscuration in the MODIS snow data product. In *59th Eastern Snow Conference*, 5–7 June 2002, Stowe, VT, 8 p. Available online at: http://modis-snow-ice.gsfc.nasa.gov/uploads/pap_cloud_obs02.pdf (accessed 28 March 2012).

Rome-Gaspaldy, S. and Ronchail, J., 2005, La pluviométrie au Pérou pendant les phases ENSO et LNSO. Available online at: http://www.ifeanet.org/publicaciones/boletines/27%283%29/675.pdf (accessed 9 February 2011).

Sidjak, R.W. and Wheate, R.D., 1999, Glacier mapping of the Illecillewaet Icefield, British Columbia, Canada, using Landsat TM and digital elevation model data. *International Journal of Remote Sensing*, **20**, pp. 273–284.

Sigurdsson, O. and Jónsson, T., 1995, Relation of glacier variations to climate changes in Iceland. *Annals of Glaciology*, **21**, pp. 263–270.

Silverio, W., 2001, Elaboration d'un SIG pour la gestion d'une zone protégée de haute montagne: application au Parc national Huascarán, Pérou. Validation memoir, post graduate certificate in geomatics, University of Geneva, Switzerland.

Silverio, W. and Jaquet, J.-M., 2003, Cartographie provisoire de la couverture du sol du Parc national Huascarán (Pérou), à l'aide des images TM de Landasat. *Télédétection*, **3**, pp. 69–83.

Silverio, W. and Jaquet, J.-M., 2005, Glacial cover mapping (1987–1996) of the Cordillera Blanca (Peru) using satellite imagery. *Remote Sensing of Environment*, **95**, pp. 342–350.

Silverio, W. and Jaquet, J.-M., 2009, Prototype land-cover mapping of the Huascarán Biosphere Reserve (Peru) using a digital elevation model, and the NDSI and NDVI indices. *Journal of Applied Remote Sensing*, **3**, 0335516, doi:10.1117/1.3106599.

Sturm, M., Hall, D.K., Benson, C.S. and Field, W.O., 1991, Non-climatic control of glacier-terminus fluctuations in the Wrangell and Chugach Mountains, Alaska, U.S.A. *Journal of Glaciology*, **37**, pp. 348–356.

Vuille, M. and Bradley, R., 2000, Mean annual temperature trends and their vertical structure in the tropical Andes. *Geophysical Research Letters*, **27**, pp. 3885–3888.

Vuille, M., Bradley, R., Werner, M. and Keimig, F., 2003, 20th century climate change in the tropical Andes: observations and model results. *Climatic Change*, **59**, pp. 75–99.

Williams Jr., R.S., Hall, D.K. and Benson, C.S., 1991, Analysis of glacier facies using satellite techniques. *Journal of Glaciology*, **37**, pp. 120–128.

Williams Jr., R.S., Hall, D.K., Sigurdsson, O. and Chien, J.Y.L., 1997, Comparison of satellite-derived with ground-based measurements of the fluctuations of the margins of Vatnajökull, Iceland, 1973-92. *Annals of Glaciology*, **24**, pp. 72–80.